

# 1 **Assessing the quality of Digital Elevation Models obtained** 2 **from mini-Unmanned Aerial Vehicles for overland flow** 3 **modelling in urban areas**

4  
5 **J. P. Leitão<sup>1</sup>, M. Moy de Vitry<sup>1</sup>, A. Scheidegger<sup>1</sup> and J. Rieckermann<sup>1</sup>**

6 [1]{Eawag: Swiss Federal Institute of Aquatic Science and Technology. Überlandstrasse 133,  
7 8600 Dübendorf, Switzerland}

8 Correspondence to: J. P. Leitão (joaopaulo.leitao@eawag.ch)

## 9 10 **Abstract**

11 Precise and detailed Digital Elevation Models (DEMs) are essential to accurately predict  
12 overland flow in urban areas. Unfortunately, traditional sources of DEM, such as airplane  
13 LiDAR DEMs and point and contour maps, remain a bottleneck for detailed and reliable  
14 overland flow models, because the resulting DEMs are too coarse to provide DEMs of  
15 sufficient detail to inform urban overland flows. Interestingly, technological developments of  
16 Unmanned Aerial Vehicles (UAVs) suggest that they have matured enough to be a  
17 competitive alternative to satellites or airplanes. However, this has not been tested so far. In  
18 this this study we therefore evaluated whether DEMs generated from UAV imagery are  
19 suitable for urban drainage overland flow modelling. Specifically, fourteen UAV flights were  
20 conducted to assess the influence of four different flight parameters on the quality of  
21 generated DEMs: i) flight altitude, ii) image overlapping, iii) camera pitch and iv) weather  
22 conditions. In addition, we compared the best quality UAV DEM to a conventional Light  
23 Detection and Ranging (LiDAR)-based DEM. To evaluate both the quality of the UAV DEMs  
24 and the comparison to LiDAR-based DEMs, we performed regression analysis on several  
25 qualitative and quantitative metrics, such as elevation accuracy, quality of object  
26 representation (e.g., buildings, walls and trees) in the DEM, which were specifically tailored  
27 to assess overland flow modelling performance, using the flight parameters as explanatory  
28 variables. Our results suggested that, first, as expected, flight altitude influenced the DEM  
29 quality most, where *lower flights* produce better DEMs; in a similar fashion, *overcast* weather

1 conditions are preferable, but weather conditions and other factors influence DEM quality  
2 much less. Second, we found that for urban overland flow modelling, the UAV DEMs  
3 performed competitively in comparison to a traditional LiDAR-based DEM. An important  
4 advantage of using UAVs to generate DEMs in urban areas is their flexibility that enables  
5 more frequent, local and affordable elevation data updates, allowing, for example, to capture  
6 different tree foliage conditions.

7

## 8 **1 Introduction**

### 9 **1.1 Urban drainage modelling**

10 Densely urbanised areas, where most economic activities take place, face higher probability  
11 of flood occurrence due to: (i) the large percentage of impervious areas, which consequently  
12 increase the runoff volume; and (ii) alterations of natural water streams and existence of  
13 sewer systems which increase flow velocities, thus reducing catchments' time of concentration  
14 and duration of the critical rainfall events. In addition, climate change may increase rainfall  
15 intensity and frequency in some regions of the Globe, which will affect ecosystems and  
16 human life. These more frequent extreme conditions can ultimately increase the probability  
17 that urban drainage system capacity is exceeded, which may lead to higher urban flood risks  
18 (when flood consequences are maintained).

19 Hydrological and hydraulic models are important tools to estimate urban flood risk and help  
20 engineers and decision makers designing urban drainage systems that inherently reduce these  
21 risks. Urban drainage models should be represented by coupling the sewer system (one-  
22 dimensional model, 1D) with the overland flow system (1D or two-dimensional models, 2D).  
23 Several studies have tested and compared different urban drainage modelling approaches (e.g.  
24 Apel et al., 2009; Villanueva et al., 2008; Allitt et al., 2009), such as 1D sewer system (e.g.,  
25 Vojinović and Tutulić, 2009), coupled 1D sewer system with 1D overland flow system  
26 (1D/1D) (e.g., Maksimović et al., 2009; Leandro et al., 2009) and coupled 1D sewer system  
27 with 2D overland flow system (1D/2D) (e.g., Chen et al., 2007). The different coupled  
28 modelling approaches rely on the quality of the Digital Elevation Model (DEM) to represent  
29 the terrain and then locate flood-prone areas – this is especially important for local (and more  
30 frequent) floods when compared to large floods (e.g., fluvial, coastal flooding, or a  
31 combination of these two types).

## 1 **1.2 UAV applications and operational challenges**

2 Unmanned Aerial Vehicles (UAVs) are uninhabited aircrafts that are reusable; thereof their  
3 operation can be either autonomous, remote controlled, or a combination of the two. The  
4 range of applications of UAVs in the civil context is already vast, e.g., archaeology (Sauerbier  
5 and Eisenbeiss 2010), precision agriculture (Zhang and Kovacs, 2012) and crowd monitoring  
6 (Duives *et al.*, 2014). UAVs have however a strong negative connotation which has motivated  
7 both civilian and military sectors to propose alternative names, such as Remotely Piloted  
8 Aircraft (RPA) or Unmanned Vehicle System (UVS) (Bennett-Jones, 2014; Eisenbeiss,  
9 2009). While their application in military operations was perhaps their first use, the industry  
10 of civil UAVs has been increasing steadily, as illustrated by the number of civil UAVs that  
11 has more than doubled since 2008 (Colomina and Molina, 2014). Applications of UAVs are  
12 also getting significant visibility in the media, mostly due to privacy (Vilmer, 2015; Wildi,  
13 2015) and safety issues.

14 UAVs can take the form of single- or multiple-blade helicopters and fixed-wing aircraft,  
15 though other possibilities exist. Eisenbeiss (2009) gives an extensive historical background of  
16 the various UAV types. These different UAV forms incorporate different safety features in  
17 order to prevent injuries and damages in the event of a flight failure; these are for example,  
18 the incorporation of a parachute. In the case of the eBee UAV, used in this study, its  
19 extremely light frame and its gliding capability make it safe in the case of flight failure and  
20 hence safe to fly in urban areas. This safety issue is of course a serious concern of the public  
21 and of the managers of public space. To respond to this concern, different countries have  
22 legislation already in place or being prepared to regulate the public use of UAVs in urban  
23 areas and mass gathering events. Nevertheless, we consider that the use of UAVs for civil  
24 applications will continue to increase, thanks to the development and improvement of the  
25 unmanned aerial systems technology such as UAV, UAV control and navigation software,  
26 and sensor technology.

## 27 **1.3 Urban drainage models input elevation data and UAVs**

28 From the literature, it is clear that a great effort has been made to develop new and improve  
29 existing numerical methods for hydraulic models. However, DEMs, as all input data, can also  
30 have a significant impact on overland flow modelling results (Fewtrell *et al.*, 2011; Leitão *et*  
31 *al.*, 2009). Leitão *et al.* (2009) showed the effect that DEM sources, resolution and accuracy

1 have on the delineation of overland flow paths in urban catchments; fine resolution DEMs are  
2 required to obtain accurate 1D overland flow networks in urban areas. Fewtrell et al. (2011)  
3 who evaluated two different hydraulic models on a DEM of resolution varying from 0.5 to  
4 5 m, also concluded that the data resolution has a greater effect on results than the model  
5 used, especially if not calibrated. While it is evident that the representation of roads is critical,  
6 requiring a minimum resolution of 2 to 3 m, walls and street curbs are also elements that  
7 influence the propagation of a flood wave (Sampson et al., 2012), but to represent these  
8 elements in the DEM, a finer resolution ( $< 1$  m) is required. Realistic and detailed  
9 representation of terrain plays thus a fundamental role in overland flow modelling.

10 The recent developments of UAVs and their increasing availability make them a new  
11 potential source of terrain elevation data. The fine spatial resolution than can be obtained  
12 (e.g., 0.05 m) is well-suited to conduct detailed urban overland flow studies. Furthermore,  
13 thanks to the low cost of operation, UAVs make multiple flights feasible, thereby enabling the  
14 analysis of how different conditions, such as tree-leaves-off or tree-leaves-on conditions,  
15 affect the characterisation of impervious areas, which is important for urban flood modelling.  
16 The handling of UAVs is simplified to a degree that can be managed by non-expert  
17 professionals, such as civil engineers and engineering consultants. To our knowledge, this  
18 study is the first time DEMs produced with photogrammetry utilising UAV imagery  
19 (commonly called UAV photogrammetry) are used in the context of urban drainage, more  
20 specifically on overland flow modelling. Although experiments have been carried out using  
21 LiDAR mounted on quadcopter-type of UAVs, this is still not possible with the eBee-UAV  
22 used in this study. Besides the issue of proprietary firmware, LiDAR equipment is heavier and  
23 consumes much more power than a camera needed to achieve similar resolution with  
24 photogrammetry. This makes it impractical when surveying significant areas of land (i.e. up  
25 to a few square kilometres for suburban catchments in Switzerland), besides increasing the  
26 safety hazard in case of a crash.

## 27 **1.4 Generation of very fine-resolution digital elevation models using UAV** 28 **imagery**

### 29 1.4.1 Photogrammetric process

30 Photogrammetry is often the preferred methodology when collecting three-dimensional (3D)  
31 data using UAVs. Photogrammetry produces 3D point clouds based on overlapping images.

1 Other useful by-products can be derived, such as urban façade textures (Leberl et al., 2010).  
2 For UAV's, photogrammetry is an interesting alternative to the predominant LiDAR (Light  
3 Detection and Ranging) method. LiDAR techniques are precise and allow for multi-returns –  
4 e.g., in areas with trees the ground elevation can be automatically measured. However, due to  
5 the weight and high-energy demand of LiDAR devices, there are not adequate for UAVs and  
6 impossible to use with mini-UAVs. On the other hand, the images can be taken with light  
7 equipment (e.g. consumer cameras) that does not require high energy. The question of  
8 photogrammetry versus LiDAR has been raised and discussed in a few past publications  
9 (Baltsavias, 1999; Leberl et al., 2010; Strecha et al., 2011). Specific applications of UAV  
10 photogrammetry are presented in Remondino et al. (2011).

11 The main photogrammetry steps to generate 3D elevation models from overlapping images  
12 are presented in Strecha et al. (2011):

- 13 1. Images are scanned for characteristic points, such as, for example, marks created in  
14 the ground specifically to support the survey or manholes. If Ground Control Points  
15 (GCPs) are used to geo-reference the model, they are usually labelled in the images  
16 before this step.
- 17 2. Based on the characteristic points, image geo-information and the known camera  
18 parameters, a sparse point cloud model is derived with a so-called bundle block  
19 adjustment algorithm (Triggs et al. 2000). It is sparse since formed only of the  
20 characteristic points from step 1.
- 21 3. Based on the sparse point cloud, dense image matching is performed to increase the  
22 spatial resolution of the point cloud model and the 3D elevation model generated.

#### 23 1.4.2 Digital Elevation Model generation process

24 The resulting point cloud may contain errors, such as image shadows, mismatches and lens  
25 distortion. Therefore, algorithms for outlier removal and smoothing can be applied. If a  
26 Digital Surface Model (DSM) is required, vegetation, buildings, and other objects need to be  
27 filtered out. Finally, the resulting point cloud is triangulated to a triangulated irregular  
28 network (TIN), which may then be rasterised and used, for example, in hydraulic modelling  
29 software.

## 1 **1.5 Study objectives**

2 In this paper we aim at demonstrating the benefit of using high-resolution DEMs produced  
3 from mini-UAV acquired data on urban drainage modelling, as opposed to DEMs based on  
4 standard aerial LiDAR elevation data. Specifically, our study presents three distinct novelties.

5 • First, to the best of our knowledge, it uses for the first time DEMs produced from  
6 UAV photogrammetry in the context of urban drainage – more specifically on  
7 overland flow modelling.

8 • Second, it presents dedicated field experiments specifically tailored to understand how  
9 UAV flight parameters affect DEM quality and, eventually, overland flow  
10 representation.

11 • Third, it compares the quality of the UAV obtained DEM with a DEM used by Swiss  
12 engineers (LiDAR-based DEM) and discusses advantages and disadvantages for urban  
13 drainage and flood modelling.

14 Our results suggested that UAVs are a very promising technology for our purpose and that  
15 results are relatively robust to not optimal flight parameters. Given the current developments,  
16 we expect that the quality of the products generated using these systems will quickly improve  
17 in the near future due to better software that manufacturers provide together with the UAV  
18 platforms. However, important limitations might arise from regulatory affairs. This will also  
19 be discussed below.

20 This paper is organised as follows: Section 2 describes the methods proposed in this study to  
21 evaluate the UAV DEM and assess the impact of flight parameters on DEM quality. In  
22 Section 3 the case study location and the flight parameters are presented; UAV and camera  
23 used are also described in this section. Analysis of findings are presented and discussed in  
24 Section 4. Finally, Section 5 summarises the major findings of the study, identifying also  
25 potential further research.

26

## 1 2 Methods

### 2 2.1 Impact of UAV flight parameters on DEM generation for overland flow 3 modelling

4 The adequacy of a DEM for urban urban flood assessment cannot be defined objectively as  
5 the existing criteria (e.g., elevation, slope or aspect differences to a benchmark DEM) are not  
6 specific to each of the possible DEM applications. As a pragmatic solution, we propose a set  
7 of four qualitative and four quantitative evaluation metrics to evaluate the DEM quality. First,  
8 DEM values were compared with field measurements using, for example mean absolute  
9 errors and visual classification. Second, two statistical models were developed to explore the  
10 relations between the flight parameters and the DEM quality through the evaluation metrics:  
11 i) an odds logistic regression model was applied for the qualitative metrics and ii) a linear  
12 regression model was used to evaluate the quantitative metrics.

#### 13 2.1.1 Qualitative metrics to assess DEM for overland flow modelling

14 *Representation of voids between two closely located objects.* This metric describes the space  
15 between two closely placed objects, such as buildings. This is an essential feature of a good-  
16 quality DEM for overland flow modelling, as in many flood events water flows through such  
17 small openings, which, consequently, can have a significant impact on the modelling results.

18 *Quality of building edges representation.* Building edges can be subject to distortions and to a  
19 “salt and pepper” effect caused by multiple 3D points being identified one over the other; this  
20 is commonly associated with pixel-based classifications (de Jong *et al.*, 2001). This metric  
21 describes the severity of building wall distortion and is important to assess the quality of the  
22 representation of linear features in the DEM which can divert overland flow.

23 *Representation of walls.* Walls are very relevant for overland flow modelling because they  
24 can obstruct and redirect water movement. This metric describes to what extent these  
25 elements are represented in the DEM.

26 *Presence of trees.* This metric describes whether trees are represented in the DEM, or not. It is  
27 desirable not to have trees represented because tree canopies, which are what is represented in  
28 the DEMs, do not influence overland flow.

1 The qualitative metrics were calculated based on a visual analysis of the DEM; a class was  
2 assigned to each analysis location. The classes are on an ordinal scale, where class 0 is the  
3 least favourable and class 3 the best class (Table 1).

4

#### 5 2.1.2 Quantitative metrics to assess DEM for overland flow modelling

6 The following quantitative metrics may be considered a first attempt to define objective  
7 evaluation criteria to assess DEM quality for overland flow modelling. The metrics aim at  
8 describing the deviations from the reality of the representation of terrain features that may  
9 influence overland flow.

10 *Absolute elevation differences.* The vertical correctness of the DEM is relevant for urban  
11 drainage modelling. Suitable reference elevation data can be surveying points and a sewer  
12 manhole cadastre. In our case study, the vertical precision of the surveying points was given  
13 for each point and varied between 0.5 and 3 cm ( $1\sigma$ ). The vertical accuracy of the manholes is  
14 not known; however, it is assumed to have a standard deviation of 7.5 cm (VBS, 2008).

15 *Curb height differences.* The height difference between road and sidewalk is relevant for  
16 relatively low overland flow. Despite runoff occurs all over the catchment area, overland flow  
17 tends to concentrate in roads in urban areas; for large runoff events (e.g. flooding events) the  
18 overland flow will flow over sidewalks. Curb heights can be measured repeatedly at various  
19 locations in the area of study. To assess the curb height from the different DEMs representing  
20 different flight parameters, the average elevation difference between 1 m<sup>2</sup> areas on the road  
21 and on the sidewalk close to the curb height measurement location was calculated.

22 *Flow direction (i.e. terrain aspect).* Flow direction was measured on the field by pouring  
23 water and measuring orientation of flow direction with a compass (see Figure 1a). In the  
24 DEM, the aspect was calculated, based on a 3x3 cell moving window (Burrough and  
25 McDonnell, 1998).

26 *Flow path delineation.* It is important that delineated flow paths are properly represented  
27 (mainly along the side of the roads), so that modelled overland flow runs into (or pass by in  
28 the vicinity of) sewer inlets. To assess the representativeness of the DEM-based delineated  
29 flow paths, real flow paths were observed by pouring water onto the road (Figure 1a) and  
30 measuring the distance between the stabilized flow and the road curb (ⓐ in Figure 1b). Often,

1 the water flowed exactly on the side of the road. In the DEM, water flow paths were estimated  
2 using the flow accumulation method (Jenson and Domingue, 1988).

3

### 4 2.1.3 Statistical models

5 To identify the important flight parameters that determine DEM quality, two simple statistical  
6 models were used; one for the qualitative and a different one for the quantitative assessments.

7 Because the qualitative metrics are measured on an ordinal scale, the influence of the flight  
8 parameters was investigated with a proportional odds logistic regression model (see, e.g.,  
9 Venables and Ripley, 2002). This model considers the natural order of the metrics, e.g. that  
10 class 3 is better than class 2. The probability that the  $j$ th observation of metric  $Y$  is at least as  
11 good as class  $k$  is modelled as

$$12 \quad P(Y_j \leq k) = \frac{1}{1 + \exp(\zeta_k - \eta_j)} \quad (1)$$

13 where the thresholds  $\zeta_0 = -\infty < \zeta_1 < \dots < \zeta_4 = \infty$  are coefficients that are estimated  
14 additionally to the *coefficients* of the linear predictor  $\eta_j$  which is defined in Eq. (2).

15 For every quantitative metric, a linear regression model was setup to model the absolute  
16 differences between the values obtained from the DEM and the corresponding ones measured  
17 in the field

$$18 \quad \eta_j = \beta_0 + \beta_1 z_{j1} + \beta_2 z_{j2} + \dots + \beta_r z_{jr} \quad (2)$$

$$19 \quad Y_j = \eta_j + \epsilon_j \quad (3)$$

20 where  $z_{jr}$  are the corresponding explanatory variables for the  $j$ th observation,  $\epsilon$  is a Gaussian  
21 random error term and the  $\beta_r$ ,  $r = 0, 1, \dots, r$  regression coefficients to be estimated. As  
22 explanatory variables all five flight parameters i) flight altitude, ii) camera pitch, iii) frontal  
23 and iv) lateral overlap, and v) weather conditions (see Section 3.3) were used. As the *weather*  
24 *condition* provides qualitative information, it was included using dummy variables (see, e.g.,  
25 Montgomery *et al.*, 2012).

## 26 2.2 Comparison between a UAV DEM and a conventional LiDAR-based DEM

27 UAV systems are being used for relatively localised surveys, and these surveys are usually  
28 targeted to a specific application. The resolution of the imagery produced using UAVs is, in

1 general, of very-high resolution as the flying altitude is low. In the specific case of this study,  
2 the UAV DEM was generated based on photogrammetry. The LiDAR-based DEM used in  
3 this study covers the whole Switzerland and was obtained to be applied in multiple purposes.  
4 By definition, the flight altitude is much higher than that of the UAV, allowing to cover larger  
5 areas in a reasonable amount of time. The LiDAR-based DEM was generated based on  
6 LiDAR technology, which is completely different from photogrammetry technique used to  
7 generate the UAV DEM.

8 From the general description above, one can say that the DEMs used for the comparison have  
9 distinct characteristics. However, the DEM comparison performed in this study is still valid as  
10 the analysis conducted in the study aims at comparing the two by practical use in engineering  
11 projects and not by technological standards or DEM generation methodologies.

12 The UAV DEM was generated based on flight 4 data (see Table 2), after a thorough  
13 comparison of the different flights (Moy de Vitry, 2014), which showed the good quality of  
14 the DEM produced from this flight. The LiDAR DEM is a 3D height model that covers the  
15 whole of Switzerland at a resolution of one data point per 2 m<sup>2</sup> and was then interpolated  
16 from the raw model to generate a 2 m raster grid. It is provided by Swisstopo<sup>1</sup> and represents  
17 all stable and visible landscape elements such as soil, natural cover, woods and all sorts of  
18 built infrastructure, such as buildings. The data acquisition method used is aerial LiDAR with  
19 a vertical accuracy of  $\pm 0.5$  m ( $1\sigma$ ) in open terrain, and in terrain with vegetation the vertical  
20 accuracy is  $\pm 1.5$  m ( $1\sigma$ ). The smallest UAV DEM pixel size was 5 cm, whereas the LiDAR  
21 DEM<sup>2</sup> had a pixel size of 2 m. Swisstopo LiDAR data is acquired in mid-summer, but the  
22 detailed processing method of the data for creating the LiDAR DEM is not published.

23 To compare the two DEMs, we built on the work of Podobnikar (2009), who discuss various  
24 visual assessment methods for identifying problems in DEMs that are otherwise not  
25 measured, like discontinuities. We also used suggestions by Reinartz *et al.* (2010) who used  
26 elevation differences and several terrain properties, like slope and land cover to compare two  
27 DEMs. Specifically, we used the following metrics for this specific purpose:

28 a. Visual DEMs comparison with hillshade<sup>3</sup>;

---

<sup>1</sup> [http://www.swisstopo.admin.ch/internet/swisstopo/en/home/products/height/dom\\_dtm-av.html](http://www.swisstopo.admin.ch/internet/swisstopo/en/home/products/height/dom_dtm-av.html)

<sup>2</sup> Swiss Federal Office of Topography (Article 30, Geoinformation Ordinance)

<sup>3</sup> A hillshade is a greyscale visualization of the 3D surface, with a lateral light source.

- 1 b. Elevation differences between the two DEMs for diverse land uses (absolute  
2 differences and mean absolute differences);
- 3 c. Slope and aspect differences between the two DEMs. These two terrain surface  
4 characteristics are essential when considering overland flow modelling as they are  
5 associated with flow speed and direction, respectively, and
- 6 d. Delineation of flow paths. The flow paths were delineated using the D8 flow  
7 direction algorithm (Jenson and Domingue, 1988). This metric is meant to help  
8 understanding the correctness of overland flow representation.

9 To compute the values for metrics (b) and (c), the 2 m downsampled UAV DEM was used to  
10 match the resolution of the LiDAR DEM used in the comparison.

### 12 **3 Material: UAV and case study**

#### 13 **3.1 Unmanned Aerial System**

##### 14 **3.1.1 General**

15 The mini-UAV platform, called “eBee”, (from year 2013) developed by senseFly was used in  
16 this study. The eBee UAV is a fully autonomous fixed-wing electric-powered aircraft, with a  
17 wingspan of 0.96 m and weighs approximately 0.7 kg including a payload of 0.15 kg. The  
18 UAV can cover relatively large areas in a reasonable amount of time (maximum of 12 km<sup>2</sup>  
19 per 50-min flight – this value is strongly related to flight altitude and, consequently, to  
20 maximum image resolution), which is important for the economic viability of UAV remote  
21 sensing. Detailed information about the UAV used in this study is presented in Appendix A.

22 We selected this specific Unmanned Aerial System over other platforms for two main  
23 reasons. First, it is delivered as a complete system with flight planning and photogrammetry  
24 software, designed to work seamlessly with one another in a straightforward and intuitive way  
25 and does not requiring flying expertise. Second, the construction of the UAV itself provides  
26 passive safety, because it is lightweight and electric powered, has a foam body and, most  
27 important, glides if out of power. In addition, the autopilot has built-in safety procedures;  
28 which is crucial for flights over urban areas.

### 1 3.1.2 Camera

2 The UAV was equipped with a customised Canon IXUS 127 HS that is triggered by the UAV  
3 autopilot. The camera has 16.1 Million Pixels with RGB bands and operates in auto mode,  
4 meaning that the photo exposure (e.g., speed and aperture) is automatically adjusted for each  
5 photo. Thus, it is not possible to configure the settings globally for a given flight; for that, a  
6 different camera would be required. Detailed characteristics of the camera are presented in  
7 Appendix A. With the eBee system, flight altitude is the main modulator for the ground  
8 sampling distance of images acquired. In Table 2 below, the reader can appreciate how flight  
9 altitude and GSD are related.

### 10 3.1.3 Photogrammetry software

11 The photogrammetry tasks, such as bundle block adjustment, point cloud generation and  
12 filtering were performed using the *Pix4D<sup>4</sup> software* (Strecha *et al.*, 2011). This is one of the  
13 leading software for UAV photogrammetry (Sona *et al.*, 2014); its main strength is a good  
14 handling of rather imprecisely referenced images like those acquired from lightweight UAVs.

## 15 3.2 The case study area

16 Adliswil is a city near Zurich (Switzerland) and was chosen to be the case study area mainly  
17 because (i) it is a typical, rapid growing Swiss city (approx. 20,000 inhabitants) that (ii)  
18 needed up-to-date elevation data to be used in other urban drainage studies. Six areas in  
19 Adliswil were initially considered and evaluated to conduct the UAV flights. The  
20 experimental area was selected based on several criteria related to overland flow, such as  
21 including different road types and sidewalks, different terrain types, significant terrain  
22 elevation difference, high road density and roads that are relatively free of cars. In addition,  
23 practical criteria, such space for UAV taking-off and landing, visibility of UAV during flight  
24 from the take-off point had to be considered. The chosen location has an area 0.04 km<sup>2</sup>  
25 (approx. 130x300 m) and is illustrated in Figure 2. The case study location is outside the  
26 Swiss Air controlled zone<sup>5</sup>, hence no permission was required to fly the UAV, as long as it  
27 always remained in line-of-sight.

---

<sup>4</sup> <http://pix4d.com/>

<sup>5</sup> <http://www.skyguide.ch>

### 1 **3.3 Experimental field work: flights with different parameters**

2 In total, 14 flights were conducted (flights 1 to 14) on the case study area to test the influence  
3 of flight parameters on the adequacy of DEMs for overland flow modelling. The flight  
4 parameters considered in this study are presented as follows.

5 *Flight altitude.* The flight altitude is one of the main factors that determines the scale and  
6 accuracy of the point cloud (Kraus 2012); it is directly related to the Ground Sampling  
7 Distance (GSD). Therefore it is expected that a low flight altitude will have a positive  
8 influence on the representation of the terrain details on DEMs. In theory, flight heights of up  
9 to 1,000 m are possible with the eBee. There is no lower limit, although safety and image  
10 overlap (the camera frequency is limited) become issues below 70 m above ground. In  
11 Switzerland, line-of-sight flight is required by the legislation, which limits the maximum  
12 altitude that is typically reached in flight.

13 *Camera pitch.* Camera pitch can be assumed to have influence on the representation of steep  
14 surfaces; high values of camera pitch are assumed to generate better representations of steep  
15 surfaces, such as façades. While façades are of limited interest in urban drainage modelling, it  
16 is of interest to see whether camera pitch variation affects the representation of objects, such  
17 as cars or walls, which influence overland flow. With the eBee, the camera pitch can be  
18 defined between 0 and 15°.

19 *Image overlap.* Image overlap is expressed in percent for both frontal and lateral directions,  
20 and is an important parameter in the photogrammetric process. First, a high overlap increases  
21 redundancy of point identification, which improves the 3D precision of the point cloud.  
22 Second, it reduces distortions in the orthophoto. In order to achieve acceptable matching  
23 between images, it is recommended to have a frontal overlap of 60% or more. This lower  
24 limit should be increased in the case of complex terrain (for example forest), or in the case of  
25 unstable platforms (for example UAVs).

26 *Weather conditions.* Lighting and the presence of shadows may have a strong effect on  
27 photogrammetry results. We deliberately did not adjust the flight plans to weather conditions.  
28 All the flights took place within a two days' time interval; some of the flights were performed  
29 under cloudy conditions whereas others were performed with direct sunlight.

30 The flights were conducted on the 29<sup>th</sup> and 30<sup>th</sup> of January 2014 between 11:30 and 13:30  
31 local time (solar noon on those days was around 12:40 local time). Additionally to the 14

1 flights, two virtual flights (flight 15 and flight 16) were generated from two of the 14 flights  
2 to simulate the effect of image overlapping. Flight 15 was generated from every third flight  
3 line of flight 14. Similarly, flight 16 was generated from every third image from flight 11.  
4 These two additional virtual flights were created to (i) increase the number of “flights” used  
5 in the statistical analysis with different parameters and (ii), specifically, to investigate the  
6 effect of image overlapping on the quality of UAV imagery DEMs. This contributed to a  
7 more robust statistical analysis of the impact of UAV flight parameters on DEM quality  
8 (based on the selected DEM evaluation metrics). The parameters of all 16 flights are  
9 presented in Table 2.

## 10 **3.4 Surveying points**

### 11 3.4.1 Georeferencing points

12 Five ground control points were used to geo-reference the digital elevation models (see Figure  
13 3). The control points used were official survey points (LFP3) with a vertical accuracy of 3.7  
14 cm and a horizontal accuracy of 3 cm. Since the points are protected with access covers, it  
15 was the access covers that were used for georeferencing the images. It was assumed that the  
16 cadastral points were directly underneath the center of their cover. For this reason, the  
17 elevation difference between the points and their covers was measured and compensated for  
18 (Figure 3), but any horizontal discrepancies were neglected.

### 19 3.4.2 Data preparation

20 The settings that were used to generate the UAV DEMs with the Pix4D software for the steps  
21 of feature extraction, point cloud generation, and point cloud filtering are shown in Table 3.  
22 The reader can refer to the Pix4D user manual (Pix4D Support Team 2014) for detailed  
23 information. For the assessment of the influence of UAV flight parameters on DEM quality,  
24 default settings were used. For the DEM comparison, settings were chosen through trial and  
25 error.

26

27 Co-registration of the UAV DEM with the LiDAR DEM is done implicitly by georeferencing  
28 the point clouds with the official survey points. By doing so, the generated UAV DEM is also  
29 georeferenced and can be directly overlaid with the LiDAR DEM, which is provided in the  
30 same coordinate reference system.

### 1 3.4.3 DEM quality assessment locations

2 Figure 4 presents the locations surveyed to then allow calculating the (a) qualitative and (b)  
3 quantitative metrics.

4

## 5 **4 Results and discussion**

6 In this section we first present the results of the influence of parameters on DEM quality, and  
7 second the results from the comparison of the UAV DEM to the LiDAR DEM.

### 8 **4.1 Impact of UAV flight parameters on DEM generation for overland flow** 9 **modelling**

10 The statistical models set up for the qualitative metrics showed that, as expected, lower flight  
11 altitude produces better DEMs for overland flow modelling; lower flights tend to increase the  
12 quality of the DEM (Figure 5a). Also, flights performed under overcast conditions led to  
13 better results (Figure 5b), most likely due to the more uniform illumination and absence of  
14 hard and moving shadows. The influences of other flight conditions are clearly not  
15 significant; Table 4 contains the summarized statistical results.

16

17 Surprisingly, none of the quantitative metrics could have been related to the flight parameters.  
18 This may indicate that the variability of the metrics between flights with the same parameters  
19 is larger than the influence of the parameters; one can also say that the performance of the  
20 UAV is robust regarding the flight configuration. The results of these statistical models are  
21 presented in Table 5 (see also the visualization in the supporting information). The significant  
22 result of the overcast weather condition for terrain elevation should not be over interpreted:  
23 first only one flight was conducted under such conditions, second the model suggest that the  
24 error is larger for overcast than for clear conditions, which is counterintuitive and contradicts  
25 the result for the qualitative metrics.

26

27 Other flight parameters than the ones considered in this study may have contributed to these  
28 results; these factors could be external, such as wind conditions and time of the day, or  
29 internal, such as the camera quality and operation mode. The camera mounted in the UAV is a

1 modified *point&shoot* consumer camera; we expect that we would have observed larger  
2 differences if a professional camera had been used. For example, a better camera could have  
3 been operated with manual exposure, settings, and would have produced more equally  
4 exposed images. This alone could have substantially improved the identification of  
5 characteristic points. These additional factors may be worth further investigations (a different  
6 experimental design) that go beyond the scope of this study.

## 7 **4.2 Comparison between UAV DEM and LiDAR DEM**

8 The objective of comparing the UAV DEMs and a nation-wide available and commonly used  
9 DEM is to evaluate whether UAV DEMs have a similar or better quality, especially in the  
10 urban areas which are relevant for overland flow modelling.

11 We expect that DEMs made available nation-wide (e.g., data sets provided by Swisstopo: the  
12 Swiss Federal Office of Topography<sup>6</sup>) are always less accurate in the vertical dimension  
13 ( $0.5 < \sigma < 1.5$  m) than the DEMs generated based on UAV imagery. Experience shows that  
14 the vertical accuracy of the latter is usually about two to three times the GSD (Pix4D Support  
15 Team 2014), which corresponds to a standard deviation of 0.1 to 0.2 m for the DEMs of our  
16 case study.

17 Because the two DEMs have different resolutions and we wanted to compare the two datasets  
18 on a pixel by pixel basis, we downscaled the UAV DEM to match the resolution of the  
19 LiDAR DEM, using the arithmetic average to compute new pixel values.

### 20 **4.2.1 Visual comparison**

21 Qualitative (visual) assessment of DEM quality can use *hillshaded* DEMs (see Figure 6).  
22 When looking into the whole area (Figures 6a and 6b), one clear difference between the two  
23 DEMs is that around the wooded ravine (marked by ①), neither the terrain nor the trees are  
24 represented in the UAV DEM. This is due to the fact that photogrammetry is ill-suited to the  
25 high spatial complexity of the trees' branches and twigs: when captured by the drone's  
26 camera from different angles, the many overlapping elements of vegetation form complex  
27 visual patterns that are specific to each point of view and therefore cannot be matched in the  
28 photogrammetric process.

---

<sup>6</sup> [www.swisstopo.ch](http://www.swisstopo.ch)

1 As a result, only a few areas below the vegetation can be regenerated in the photogrammetric  
2 point cloud. Because of the visual noise caused by overhead branches, the 3D accuracy of the  
3 point cloud in these areas is compromised, which predisposes the points to be removed during  
4 the automatic point cloud filtering process. The tree-leaves-off conditions during the UAV  
5 flight in early March makes it difficult to identify matching points in the canopy/on bare thin  
6 branches which are often less wide than the GSD. In our experiments with the image dataset,  
7 it was fully possible to reconstruct the tree trunks and branches of many of the trees in the  
8 above-mentioned area, but it required an image overlap far superior than what is common for  
9 cartographic photogrammetry missions. Not having the tree canopies represented is though  
10 not a problem for overland flow modelling.

11 Apart from differences due to the presence and better representation of vegetation in the  
12 LiDAR DEM, there are also mobile objects such as vehicles that differ between the two  
13 scenes.

14

15 When looking at the insets, it appears that the quality of the two DEMs is very similar, with  
16 the exception that the LiDAR DEM has more noise and sharper edges than the UAV DEM.  
17 This can be at least partially explained by the averaging performed when downsampling the  
18 UAV DEM.

19 Because the two DEMs represent different seasons, there are a number of differences between  
20 the two DEMs that are due to physical changes in the environment and not due directly to the  
21 characteristics of one DEM generation process or the other. Therefore, the comparison of the  
22 two elevation data sets using the whole area not meaningful. Due to this fact, the comparison  
23 of the DEMs presented in the following sections will be limited to a selected road area (area  
24 marked with the red line polygon in Figure 7). This area was defined based on visual analysis  
25 of the aerial orthophoto associated to the UAV DEM. This area covers approximately  
26 1,500 m<sup>2</sup> and his free from cars, trees and man-made elements such as constructions in both  
27 DEMS.

28

## 1 4.2.2 Elevation comparison

2 The map of the elevation differences between the UAV DEM and the LiDAR DEM  
3 (Figure 7) was calculated subtracting the LiDAR DEM from the UAV DEM (Eq. 4) with  
4 2 m pixel<sup>-1</sup> resolution.

$$5 \quad \Delta z_{ij} = UAV_{ij} - Swisstopo_{ij} \quad (4)$$

6 where  $\Delta z_{ij}$  is the elevation difference between the two DEMs in the cell  $ij$ ,  $UAV_{ij}$  represents  
7 the elevation value of the cell  $ij$  of the UAV DEM and  $Swisstopo_{ij}$  represents the elevation  
8 value of the cell  $ij$  of the LiDAR DEM.

9 As can be seen in Figure 8, the differences between the two DEMs in this area are almost  
10 negligible. The minimum, maximum, mean and standard deviation of the elevation  
11 differences between the two DEMs are -0.468 m, 0.306 m, 0.06 m and 0.119 m, respectively.

12

## 13 4.2.3 Slope and aspect comparison

14 The slope differences were calculated for the selected road area (see red line polygon in  
15 Figure 6a) using (Eq. 5) with 2 m pixel<sup>-1</sup> resolution.

$$16 \quad \Delta s_{ij} = UAV_{ij} - Swisstopo_{ij} \quad (5)$$

17 where  $\Delta s_{ij}$  is the slope difference between the two DEMs in the cell  $ij$ ,  $UAV_{ij}$  represents the  
18 slope value of the cell  $ij$  of the UAV DEM and  $Swisstopo_{ij}$  represents the slope value of the  
19 cell  $ij$  of the LiDAR DEM.

20 As can be seen in Figure 9, the slope differences between the two DEMs are almost always  
21 below 10%; it is noteworthy that the larger slope differences are located along the boundary  
22 of the red-line polygon. The value of the descriptive statistics of the slope differences between  
23 of the two DEM are:

- 24 • Minimum: -115.64%
- 25 • Maximum: 74.41%
- 26 • Mean: -0.86%, and
- 27 • Standard deviation: 14.16%.

28 The terrain aspect distribution of the selected road area of the two DEMs is also very similar,  
29 as presented in Figure 10.

1

#### 2 4.2.4 Delineation of flow paths

3 Flow paths were delineated using the conventional D8 flow direction algorithm (Jenson and  
4 Domingue, 1988) for the three UAV DEMs at different resolutions (0.5, 1.0 and 2.0 m pixel<sup>-1</sup>)  
5 as well as for the LiDAR DEM. The results are presented in Figure 11 and show that the flow  
6 paths delineated using the UAV DEMs followed a realistic path along the side of the road.  
7 This behaviour was retained even when the UAV DEM was downsampled to 2 m pixel<sup>-1</sup>  
8 (Figure 11c); this is in close agreement with the results presented by Sampson *et al.* (2012),  
9 who downsampled terrestrial LiDAR for use in urban inundation models. In comparison to  
10 the LiDAR DEM, it is clearly seen that the UAV DEMs can add additional detail to overland  
11 flow modelling applications; flow paths obtained using the LiDAR DEM are slightly different  
12 from the ones obtained using the UAV-based DEM.

13

### 14 5 Conclusions

15 In this study, we demonstrate the applicability and the advantages of using UAVs to generate  
16 very-high-resolution DEMs to be used in urban overland flow and flood modelling. To  
17 address this objective, we assessed (i) the influence of flight parameters in the quality of the  
18 DEMs produced using UAVs technology, and (ii) the quality of the UAV-based DEM in  
19 comparison to the conventional LiDAR-based DEM available in Switzerland. We concluded  
20 that:

- 21 • UAV platforms and software are a mature technology that deliver basic data leading to  
22 satisfactory results for urban overland flow modelling.
- 23 • Interestingly, only few dependencies between the flight parameters and DEM quality  
24 could be identified. This might be due to variability introduced by other external and  
25 internal factors not investigated in detail in this study. Although, at first sight, this  
26 might leave only little potential for optimal experimental design, at second sight this  
27 also means that the technology is rather robust against flight altitude, camera pitch  
28 settings, image overlapping parameters and thus suitable for practitioners.
- 29 • As expected, the most influential flight parameter was the flight altitude, where *lower*  
30 *flights* produce better DEMs. Other flight parameter, such as the effect of sun (e.g.,

1 weather conditions), showed some effect on the DEM quality but its effect was clearly  
2 weaker than the flight altitude – *overcast weather conditions* are better. Other  
3 relationships could not be observed as hypothesized, e.g., camera pitch and image  
4 overlapping. For a given flight parameter, the number of samples (flights) may have  
5 been a limiting factor to observe trends. In future studies, it would be recommended to  
6 conduct additional flight campaigns. By repeating flights with the same parameters in  
7 order to quantify how much DEM quality may vary, independently of flight  
8 parameters one may also evaluate uncertainty in the elevation data generated.  
9 Additional flight parameters may also be considered in future studies, such as time of  
10 the day.

- 11 • Comparing the UAV DEM to a commonly available LiDAR-based DEM, we found  
12 that the quality of both DEMs is comparable. The differences between the two DEMs  
13 are not substantial, especially when the comparison is conducted in a selected road  
14 area without cars, buildings, trees or vegetation. When comparing flow paths  
15 delineated using the different DEMs, it could be seen that the flow paths obtained  
16 using a DEM downsampled (2 m pixel size) from the finer resolution UAV DEM  
17 (0.05 m pixel size) retained the major flow path patterns. The flow paths obtained  
18 using the LiDAR DEM were slightly different from those obtained using the UAV  
19 DEMs; this is mostly due to the presence of vegetation and trees in the first DEM. The  
20 UAV DEM has two main/practical advantages over the LiDAR DEM, despite the  
21 similarities mentioned above. First, it is more flexible to acquire elevation data using  
22 UAVs, especially for small to medium size areas (or catchments), and the second is  
23 that if the UAV flights are conducted during winter with tree-leaves-off conditions,  
24 DEMs with no tree canopies represented can be produced, which are especially  
25 beneficial for land use classification and overland flow processes. It is however  
26 important to mention that there are other solutions to generate DEMs other than  
27 nationwide airborne LiDAR-based and UAV-based solutions, such as ground-based  
28 LiDAR. In particular, ground-based LiDAR solution is flexible too as the UAV  
29 solution, capable of producing very-fine resolution DEMs and may not have the  
30 problem of obstruction by tree-leaves as photogrammetric mini-UAV solutions.  
31 However, it also has disadvantages: the major one is perhaps related to the limitation  
32 of covering areas located behind the buildings, i.e., it does not allow for covering the  
33 whole area of interest (e.g., an urban catchment).

- 1       • Our findings suggest that UAVs can greatly improve overland flow modelling by  
2       increasing the detail of terrain representation and also by their inherent flexibility to  
3       update existing elevation datasets. The very high resolution possible to obtain using  
4       UAV DEMs is also an advantage for urban overland flow and flood modelling  
5       purposes. Further research should be carried out towards the development of an urban  
6       drainage modelling application in order to assess the real benefit of using very-high  
7       resolution DEMs and hydraulic models.

8       In addition to the generation of DEMs, UAV imagery can also be used to generate other very  
9       interesting data sets for urban drainage modelling applications based on image classification.  
10      These are, for example: identification of pervious/ impervious areas (Tokarczyk et al.,  
11      accepted); automatic identification and location of sewer inlets and manholes and other man-  
12      made features relevant to overland flow (Moy de Vitry, 2014).

## 14      **Acknowledgements**

15      The authors are grateful for the expert advice received from Prof. Konrad Schindler, ETH  
16      Zurich, during the development of this study, especially regarding photogrammetry.

## 18      **References**

- 19      Allitt, R., Blanksby, J., Djordjevic, S., Maksimovic, C., Stewart, D. (2009). Investigations  
20      into 1D-1D and 1D-2D Urban Flood Modelling. In *WaPuG Autumn conference 2009*,  
21      Blackpool, UK
- 22      Apel, H., Aronica, G. T., Kreibich, H., Thielen, A. H. (2009). Flood Risk Analyses—how  
23      Detailed Do We Need to Be? *Natural Hazards*, 49(1): 79–98. doi:10.1007/s11069-008-9277-  
24      8
- 25      Baltsavias, E. (1999). A Comparison between Photogrammetry and Laser Scanning. *ISPRS*  
26      *Journal of Photogrammetry and Remote Sensing*, 54(2–3): 83–94. doi:10.1016/S0924-  
27      2716(99)00014-3
- 28      Bennett-Jones, O. (2014). *Searching for a New Name for Drones*. BBC News.  
29      <http://www.bbc.com/news/magazine-25979068>

- 1 Burrough, P. A., McDonnell, R. A. (1988). *Principles of Geographical Information Systems*.  
2 Oxford University Press, New York.
- 3 Chen A. S., Djordjević, S., Leandro, J., Savić, D. (2007) The urban inundation model with  
4 bidirectional flow interaction between 2D overland surface and 1D sewer networks. In  
5 *Novatech*, Lyon, France
- 6 Colomina, I., Molina, P. (2014). Unmanned Aerial Systems for Photogrammetry and Remote  
7 Sensing: A Review. *ISPRS Journal of Photogrammetry and Remote Sensing*, 92: 79–97.  
8 doi:<http://dx.doi.org/10.1016/j.isprsjprs.2014.02.013>
- 9 De Jong, S.M., Hornstra, T., Maas, H. (2001). An integrated spatial and spectral approach to  
10 the classification of Mediterranean land cover types: the SSC method. *International Journal*  
11 *of Applied Earth Observation and Geoinformation*, 3(2), 176-183
- 12 Duives, D. C., Daamen, W., Hoogendoorn, S. (2014). Trajectory Analysis of Pedestrian  
13 Crowd Movements at a Dutch Music Festival. In Weidmann, U., Kirsch, U., Schreckenberg,  
14 M. (Eds.) *Pedestrian and Evacuation Dynamics 2012*. Springer International Publishing.  
15 [http://link.springer.com/chapter/10.1007/978-3-319-02447-9\\_11](http://link.springer.com/chapter/10.1007/978-3-319-02447-9_11)
- 16 Eisenbeiss, H. (2009). *UAV Photogrammetry*. Zürich: ETH Zürich Inst. f. Geodäsie u.  
17 Photogrammetrie
- 18 Fewtrell, T. J., Duncan, A., Sampson, C. C., Neal, J. C., Bates, P. D. (2011). Benchmarking  
19 Urban Flood Models of Varying Complexity and Scale Using High Resolution Terrestrial  
20 LiDAR Data. *Physics and Chemistry of the Earth, Parts A/B/C* 36(7-8): 281–91.  
21 doi:10.1016/j.pce.2010.12.011
- 22 Jenson, S. K., and J. O. Domingue (1988). Extracting Topographic Structure from Digital  
23 Elevation Data for Geographic Information System Analysis. *Photogrammetric Engineering*  
24 *and Remote Sensing*, 54(11), 1593–1600
- 25 Kraus, K. (2012). *Band 1 Photogrammetrie, Geometrische Informationen aus Photographien*  
26 *und Laserscanneraufnahmen*. Berlin, Boston: De Gruyter.  
27 <http://www.degruyter.com/view/product/61449>
- 28 Leandro, J., Djordjević, S., Chen, A., Savić, D.A. (2009). Flood inundation maps using an  
29 improved 1D/1D model. In *8<sup>th</sup> UDM: International Conference on Urban Drainage*  
30 *Modelling*, Tokyo, Japan

- 1 Leberl, F., Irschara, A., Pock, T., Meixner, P., Gruber, M., Scholl, S., Wiechert, A. (2010).  
2 Point Clouds: LIDAR versus 3D Vision. *Photogrammetric Engineering and Remote Sensing*,  
3 76: 1123–34
- 4 Leitão, J. P., Boonya-aroonnet, S., Prodanovic, D., Maksimovic, C. (2009). The influence of  
5 digital elevation model resolution on overland flow networks for modelling urban pluvial  
6 flooding. *Water Science and Technology*, 60 (12), 3137–3149. doi:10.2166/wst.2009.754
- 7 Maksimović, Č., Prodanović, D., Boonya-aroonnet, S., Leitão, J. P., Djordjević, S., Allitt, R.  
8 (2009). Overland flow and pathway analysis for modelling of urban pluvial flooding. *Journal*  
9 *of Hydraulic Research*, 47(4): 512-523. doi:10.1080/00221686.2009.9522027
- 10 Montgomery, D. C., Peck, E. A., Vining, G. G. (2012) *Introduction to Linear Regression*  
11 *Analysis*, Hoboken, NJ, Wiley. ISBN: 978-0-470-54281-1
- 12 Moy de Vitry, M. (2014). *Improving urban flood management with autonomous mini-UAVs* .  
13 MSc thesis, ETH Zurich, Zurich, Switzerland
- 14 Pix4D Support Team (2014). *Pix4D Knowledge Base. Pix4D Support*.  
15 <https://support.pix4d.com/entries/26825498>. [accessed 27 April 2015], archived by WebCite  
16 at <http://www.webcitation.org/6Y6TNZI2U>
- 17 Podobnikar, T. (2009). Methods for Visual Quality Assessment of a Digital Terrain Model.  
18 *S.A.P.I.E.N.S. Surveys and Perspectives Integrating Environment and Society*, 2.2 (May).  
19 <http://sapiens.revues.org/738>
- 20 Reinartz, P., d' Angelo, P., Krauß, T., Poli, D., Jacobsen, K., Buyuksalih, G. (2010).  
21 Benchmarking and Quality Analysis of Dem Generated from High and Very High Resolution  
22 Optical Stereo Satellite Data. In *Proceedings of the The 2010 Canadian Geomatics*  
23 *Conference and Symposium of Commission I, ISPRS Convergence in Geomatics – Shaping*  
24 *Canada's Competitive Landscape*, Calgary, Alberta, Canada [available from:  
25 [http://www.isprs.org/proceedings/XXXVIII/part1/09/09\\_03\\_Paper\\_33.pdf](http://www.isprs.org/proceedings/XXXVIII/part1/09/09_03_Paper_33.pdf)]
- 26 Remondino, F., Barazzetti, L., Nex, F., Scaioni, M., Sarazzi, D. (2011). UAV  
27 Photogrammetry for Mapping and 3d Modeling–current Status and Future Perspectives.  
28 *International Archives of the Photogrammetry, Remote Sensing and Spatial Information*  
29 *Sciences*, 38 (1/C22), 25-31, Zurich, Switzerland

1 Sampson, C. C., Fewtrell, T. J., Duncan, A., Shaad, K., Horritt, M. S., Bates, P. D. (2012).  
2 “Use of Terrestrial Laser Scanning Data to Drive Decimetric Resolution Urban Inundation  
3 Models.” *Advances in Water Resources*, 41(June): 1–17.  
4 doi:10.1016/j.advwatres.2012.02.010

5 Sauerbier, M., Eisenbeiss, H. (2010). UAVs for the Documentation of Archaeological  
6 Excavations. *International Archives of Photogrammetry, Remote Sensing and Spatial  
7 Information Sciences*, 38(Part 5), 526-531, Newcastle upon Tyne, UK

8 Sona, G., Pinto, L., Pagliari, D., Passoni, D., Gini, R. (2014). Experimental Analysis of  
9 Different Software Packages for Orientation and Digital Surface Modeling from UAV  
10 Images. *Earth Science Informatics*, 7(2): 97–107. doi:10.1007/s12145-013-0142-2

11 Strecha, C., Gervais, F., Fua, P., Zufferey, J-C., Beyeler, A., Floreano, D., Küng, O. (2011).  
12 The Accuracy of Automatic Photogrammetric Techniques on Ultra-Light UAV Imagery. In  
13 *UAV-g 2011 - Unmanned Aerial Vehicle in Geomatics*, Zurich, Switzerland. [available from:  
14 <http://infoscience.epfl.ch/record/168806>]

15 Tokarczyk, P., Leitão, J. P., Rieckermann, J., Schindler, K., Blumensaat, F. (accepted).  
16 *Hydrology and Earth System Sciences*

17 Swisstopo (2013). *SWISSIMAGE - Das Digitale Farborthophotomosaik Der Schweiz*.  
18 Eidgenössisches Departement für Verteidigung, Bevölkerungsschutz und Sport VBS.

19 VBS (2008). Technische Verordnung Des VBS Über Die Amtliche Vermessung (in German)  
20 <http://www.admin.ch/opc/de/classified-compilation/19940126/200807010000/211.432.21.pdf>  
21 retrieved on 23.04.2015.

22 Triggs, B., McLauchlan, P. F., Hartley, R. I., Fitzgibbon, A. W. (2000). Bundle Adjustment  
23 — A Modern Synthesis. In Triggs, B., Zisserman, A., Szeliski, R. (Eds.). *Vision Algorithms:  
24 Theory and Practice*. Lecture Notes in Computer Science 1883. Springer, Berlin Heidelberg.  
25 [http://link.springer.com/chapter/10.1007/3-540-44480-7\\_21](http://link.springer.com/chapter/10.1007/3-540-44480-7_21).

26 Venables, W.N., Ripley, B.D. (2002). *Modern Applied Statistics with S*. Springer, New York.  
27 ISBN: 978-0-387-95457-8

28 Villanueva, I., Pender, G., Lin, B., Mason, D. C., Falconer, R. A., Neelz, S., Crossley, A. J.,  
29 Mason, D. C. (2008). Benchmarking 2D Hydraulic Models for Urban Flooding. *Proceedings  
30 of the ICE - Water Management*, 161(1): 13–30. doi:10.1680/wama.2008.161.1.13.

- 1 Vilmer, J.-B. (2015). Armed drones and target killings: legal and ethical challenges. In  
2 *Drones: From Technology to Policy, Security to Ethics* Forum. 30 January, ETH Zurich,  
3 Switzerland
- 4 Vojinovic, Z., Tutulic, D. (2009). On the use of 1D and coupled 1D–2D modelling  
5 approaches for assessment of flood damages in urban areas. *Urban Water Journal*, 6(3): 183–  
6 199
- 7 Wildi, J. (2015). Drones: industry and business applications. In *Drones: From Technology to*  
8 *Policy, Security to Ethics* Forum. 30 January, ETH Zurich, Switzerland
- 9 Zhang, C., Kovacs, J.M. (2012). The Application of Small Unmanned Aerial Systems for  
10 Precision Agriculture: A Review. *Precision Agriculture*, 13 (6): 693–712.  
11 doi:10.1007/s11119-012-9274-5  
12

## 1 **Appendix A. Unmanned Aerial System**

2 The mini-UAV platform used in the study is a fully autonomous fixed-wing aircraft  
3 developed by senseFly SA<sup>7</sup>. The UAV is electric-powered, has a wingspan of 0.96 m, and  
4 weighs approximately 0.7 kg including a payload of 0.15 kg. The UAV can cover large areas  
5 in a reasonable amount of time, which is important for the economic viability of UAV remote  
6 sensing. Detailed information is provided in Table A1.

7 Table A1. Detailed characteristics of the UAV

---

Wingspan	0.96 m
Wing area	0.25 m
Typical Weight	0.7 kg
Payload	16 MP camera, electronically integrated and controlled
Battery	3-cell Lithium-Polymer
Capacity	1800 mAh
Endurance	45 minutes of flight time
Propulsion	Electric brushless motor
Nominal cruise speed	36-72 km h <sup>-1</sup> (10-20 m s <sup>-1</sup> )
Wind resistance	up to 45 km h <sup>-1</sup> (12 m s <sup>-1</sup> )
Mapping area	coverage up to 10 km <sup>2</sup>
Remote control	2.4 GHZ, range: approx. 1 km, certification: CE. FCC
Data communication	2.4 GHZ, range: approx. 3 km, certification: FCC Part 15.247
Navigation	Autonomous flight and landing, up to 50 waypoints direction
Material	Styrofoam
Cost (in 2015)	Approx.. CHF 20,000 (UAV + camera + software)

---

8

---

<sup>7</sup> <http://www.sensefly.com>

1 The specifications of the IXUS 127 HS camera part of the Unmanned Aerial System used in  
2 this study are presented in Table A2.

3 Table A2. Specifications of the Canon IXUS 127 HS

---

Camera effective pixels	Approx. 16.1 million pixels
Lens focal length	5x zoom: 4.3 (W) — 21.5 (T) mm (35mm film equivalent: 24 (W) — 120 (T) mm)
File formats	Exif 2.3 (JPEG)
Dimensions	93.2x57.0x20.0 mm (Based on CIPA Guidelines)
Weight	Approx. 0.135 kg (including batteries and memory card)

---

4

5

1 Table 1. Qualitative metric classes

Class	Representation of voids	Representation of buildings edges	Representation of walls	Presence of trees
3	100% open	Sharp edges	Perfectly represented wall	Not visible
2	50% open	Little noisy	A straight object	Freckles
1	25% open	Very noisy	Unclear	Almost complete
0	0% open	Chaotic	Nothing	Complete

2

1 Table 2. Characteristics of the 16 flights

Flights	Flight altitude (m)	GSD (cm)	Camera Pitch (°)	Frontal overlap (%)	Lateral overlap (%)	Weather conditions <sup>b</sup>
1	145	4.5	0	80	70	Clear
2	145	4.5	0	70	80	Clear
3	145	4.5	7	70	80	Clear
4 <sup>a</sup>	145	4.5	15	70	80	Clear
5	205	6.5	0	70	80	Clear
6	205	6.5	7	70	80	Clear
7	205	6.5	15	70	80	Clear
8	85	2.5	0	70	80	Overcast
9	310	10	0	70	80	Partly cloudy
10	220	7	5	70	80	Clear
11	220	7	5	85	80	Partly cloudy
12	220	7	5	55	80	Clear
13	220	7	5	70	65	Clear
14	220	7	5	70	90	Clear
15	220	7	5	70	70	Clear
16	220	7	5	60	80	Partly cloudy

2 <sup>a</sup> DEM generated from flight 4 was used for the comparison with the LiDAR DEM.

3 <sup>b</sup><http://www.erh.noaa.gov/er/box/glossary.htm>

4

1 Table 3. Pix4D settings that were used to generate the UAV DEM

	<b>Assessment of influence of UAV flight parameters on DEM quality</b>	<b>Comparison of UAV DEM with LiDAR DEM</b>
<b>Initial processing</b>		
Feature extraction scale	1	1
Image Re-matching	No	No
<b>Point cloud generation</b>		
Image scale	½, Multiscale	½, Multiscale
Point density	One 3D point for every 8 pixels of original image	One 3D point for every 8 pixels of original image
Minimum matches	3	4
<b>Point cloud filtering</b>		
Noise filtering radius	10 GSD	14 GSD
Surface smoothing type	<i>Sharp</i>	<i>Medium</i>
Smoothing radius	10 GSD	20 GSD

2

1 Table 4. Results of the statistical models for the qualitative metrics.

	Representation of voids		Representation of building edges		Representation of walls		Representation of trees	
	Estimated value	P-value	Estimated value	P-value	Estimated value	P-value	Estimated value	P-value
Flight altitude (m)	-0.00778	0.1554	-0.02531	<b>0.001</b>	-0.02950	<b>0.046</b>	-0.02685	<b>0.000</b>
Camera Pitch (°)	0.00046	0.9876	0.02550	0.465	-0.09347	0.215	-0.05554	0.069
Frontal overlap (%)	-0.03073	0.4775	-0.02024	0.682	-0.01141	0.901	0.00911	0.829
Weather conditions: (Overcast)	1.17177	0.2455	-0.37471	0.748	14.00542	<b>0.000</b>	15.03059	<b>0.000</b>
Weather conditions: (Partly cloudy)	0.16054	0.7792	-0.53598	0.438	-1.11497	0.419	-0.44932	0.426

2

3

1 Table 5. Results of the statistical models for the quantitative metrics.

	Terrain elevation		Curb height		Aspect		Flowpath distance	
	Estimated value	P-value	Estimated value	P-value	Estimated value	P-value	Estimated value	P-value
Flight altitude (m)	0.00011	0.629	-0.00009	0.993	0.04405	0.801	0.00153	0.497
Camera Pitch (°)	-0.00200	0.264	-0.00274	0.974	-1.04400	0.434	0.00213	0.903
Frontal overlap (%)	0.00032	0.800	-0.00027	0.996	-0.28786	0.759	-0.01938	0.117
Weather conditions: (Overcast)	0.14273	<b>0.001</b>	0.00921	0.996	-15.21044	0.629	-0.16416	0.680
Weather conditions: (Partly cloudy)	-0.00218	0.929	-0.02515	0.982	-11.16398	0.539	-0.02149	0.925

2

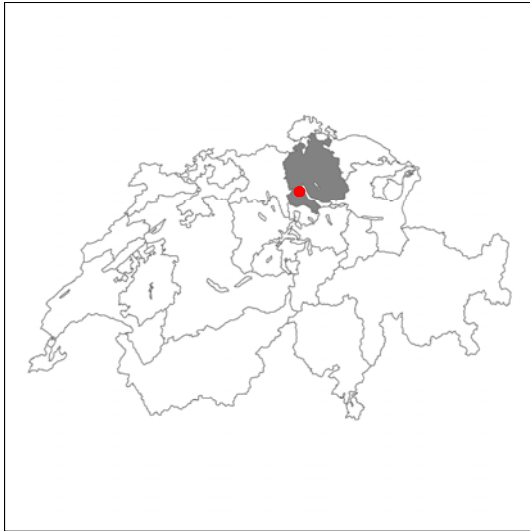


(a) Terrain aspect and Flow path field experiment preparation



(b) Aerial photo of field experiment location

- 1 Figure 1. Example of the field experiments conducted to calculate the terrain flow direction
- 2 and flow path delineation metrics



(a) Adliswil (Zurich Canton, Switzerland)



(b) Case study areal aerial photo (130x300 m)

1 Figure 2. Case study location and area aerial photo



1

2 Figure 3: Left: locations of the georeferencing points used in the study (red crosses). While

3 the left-most points are outside of the area of study, they were covered by UAV images.

4 Right: measurement of vertical distance between GCP access cover and actual GCP point.



Legend

Qualitative Assessment Regions

- Forested terrain
- Tree structure
- Building outline
- Gaps between objects
- Wall representation



Experiment locations

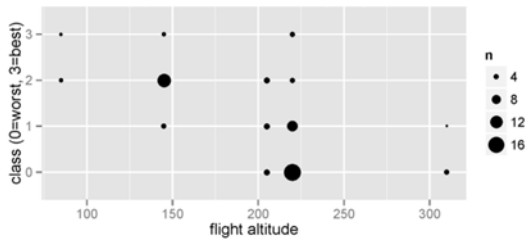
- Curb Height
- Flow Direction
- Flow Path

(a) Qualitative assessment

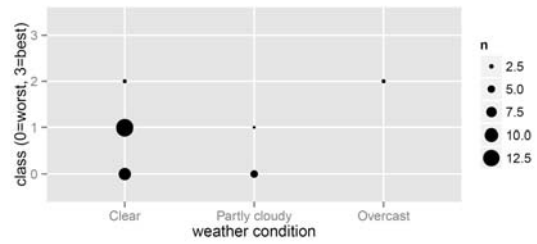
(b) Quantitative assessment

1 Figure 4. Location used to calculate the metric values

2



(a) Representation of building edges

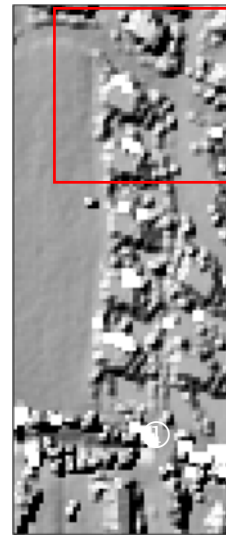


(b) Representation of walls

1 Figure 5. Relationship between the quality of the representation of building edges and flight  
 2 altitude and between wall representation and weather conditions. The size of the dots is  
 3 proportional to the number of observed metrics with identical quality class and altitude or  
 4 weather condition, respectively.



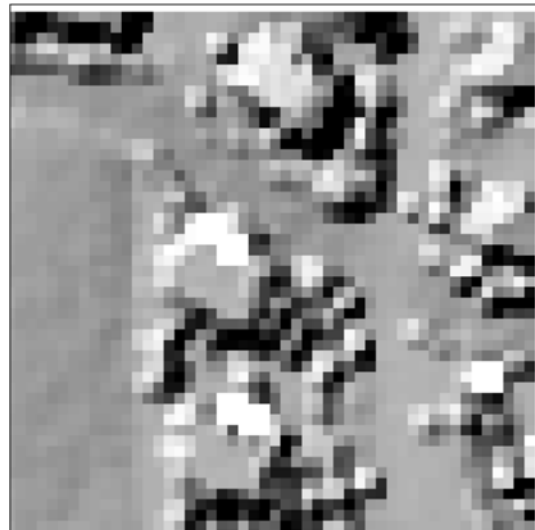
(a) UAV DEM overview (downsampled to 2 m pixel<sup>-1</sup>)



(b) LiDAR DEM overview (2 m pixel<sup>-1</sup>)



(c) UAV DEM inset (downsampled to 2 m pixel<sup>-1</sup>)

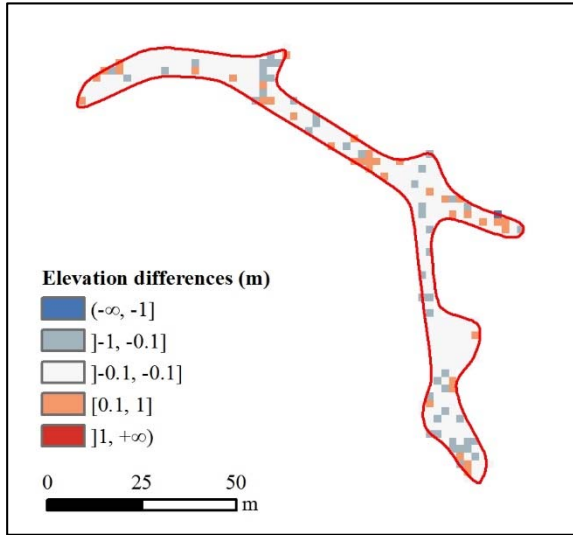


(d) LiDAR DEM inset (2 m pixel<sup>-1</sup>)

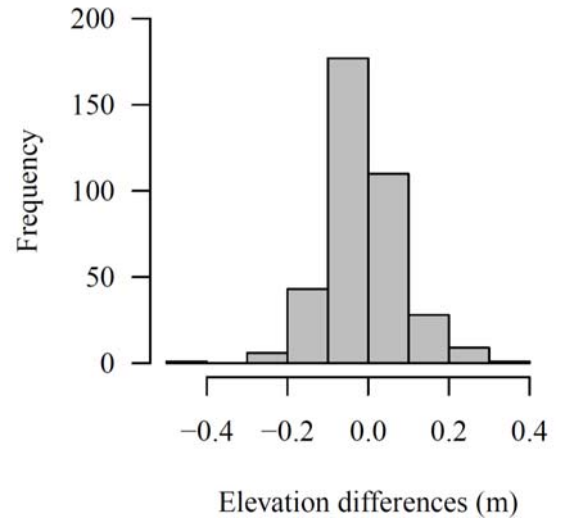
1 Figure 6. Visual comparison of the UAV DEM and LiDAR DEM.



1



(a) Spatial distribution

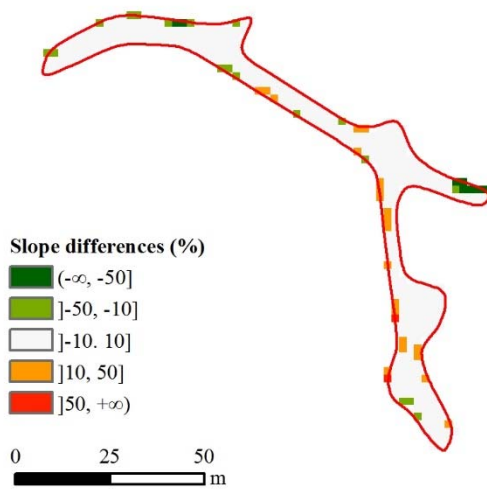


(b) Histogram

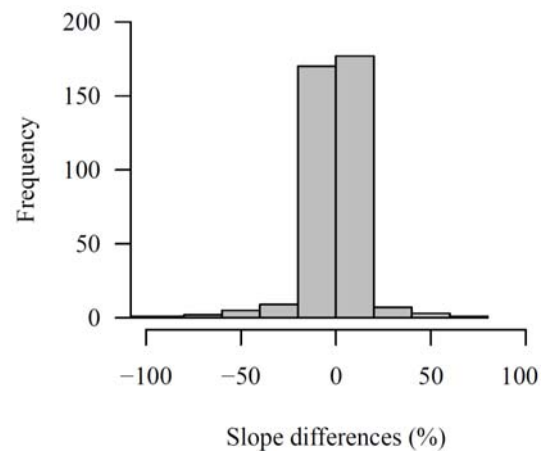
2 Figure 8. Elevation differences between the UAV DEM and the LiDAR DEM (both with  
3  $2 \text{ m pixel}^{-1}$  resolution)

4

1



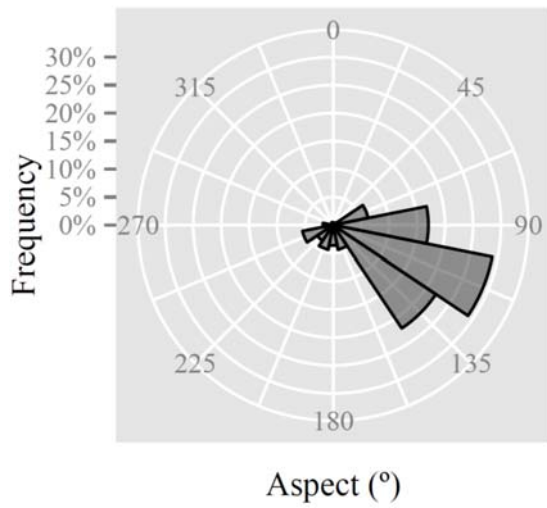
(a) Spatial distribution



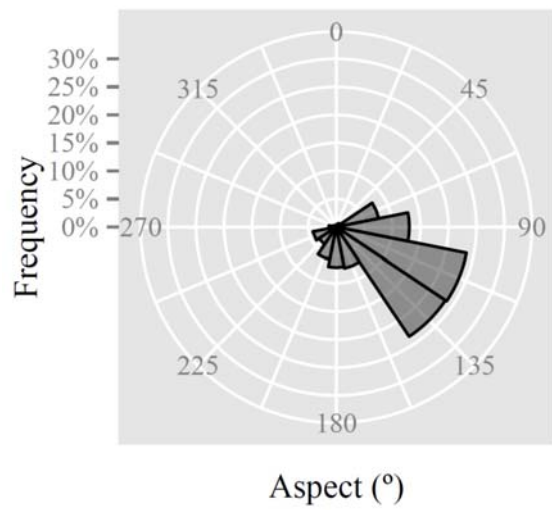
(b) Histogram

2 Figure 9. Slope differences between the UAV DEM and the LiDAR DEM

3



(a) UAV DEM



(b) LiDAR DEM

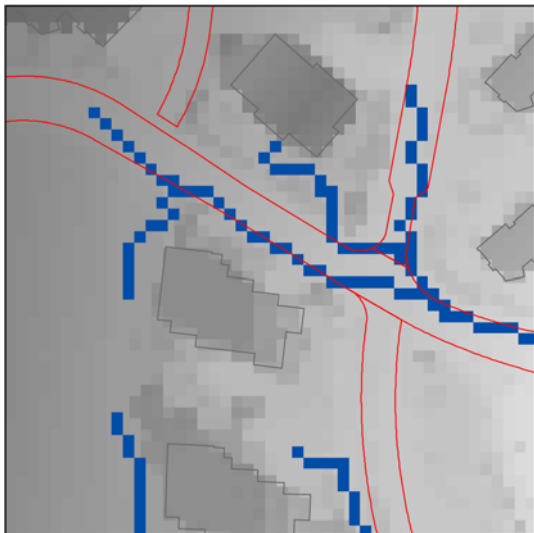
- 1 Figure 10. Distribution of terrain aspect. The aspect values are in degrees. The outer number
- 2 represent the cardinal directions in degrees.
- 3



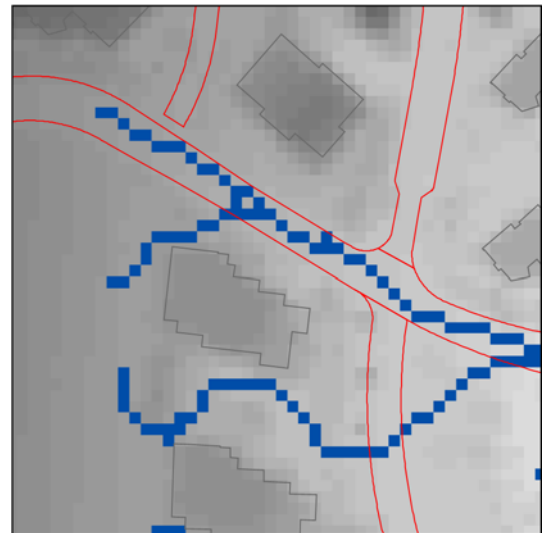
(a) UAV DEM (0.5 m pixel<sup>-1</sup>)



(b) UAV DEM (1 m pixel<sup>-1</sup>)



(c) UAV DEM (downsampled to 2 m pixel<sup>-1</sup>)



(d) LiDAR DEM (2 m pixel<sup>-1</sup>)

1 Figure 11. DEM-based flow path delineation